

Intelligent Control for Laboratory DC Motor

B. M. Mustapha, V. C. Ikpo, A. B. Bababe

Abstract- This paper presents the design of a fuzzy PD controller for laboratory DC motor (MS 150 Kit) to minimize the tracking error in applications. The Fuzzy PD controller was simulated and the responses obtained when compared with a conventional PD controller revealed better performance.

Keywords: Control, Direct-Current, Fuzzy, Motor

I. INTRODUCTION

Over time, the application of Direct-current motors has evolved resulting to designs of systems especially in power electronics advancement[1]. This is due its remarkable advantages conveyed by the portable size, high speed, safety and cost effectiveness[2]. In recent times, DC motors are predominant in most industrial applications. Some of the application areas includes the position control and speed control of computers (disk drives, printer drives), robot manipulators, servo mechanism and other industrial application projects[3]. The performance expectations of the DC motor are very high, hence demands high-performance controllers to enable it yield specific results. A major performance requirement is quick response to input command in the presence of external disturbance and efficient reduction in error signal[4]. In recent years, much research efforts have been reported in the aspect of DC Motor control owing to its importance and simplicity in many applications. However, the conventional PD controllers are not very robust to ensuring this specification is adequately tuned[5, 6]. A controller that will yield precise position and dynamic performance in terms of reduced error in trajectory tracking is essential. This paper presents the design of Fuzzy PD controller with emphasis on reference signal tracking is using bond graph. The DC motor exhibit speed torque characteristics that are preferred to AC motors[7]. Hence, the DC motor possess a speed control feature that can be adjusted manually by the operator or by means of automation[8]. The fuzzy PD result is compared against that of a conventional PD controller.

II. DC MOTOR MODELLING USING BOND GRAPH

Bond graph is domain independent technique that utilizes graphical, mathematical, algorithmic and symbolic techniques to derive the nonlinear models of a system[9].

Manuscript published on 28 February 2017.

* Correspondence Author (s)

B. M. Mustapha, Department of Electrical & Electronics Engineering, University of Maiduguri, Nigeria. Email: bgmustaphae@yahoo.com

V. C. Ikpo, Department of Electrical & Computer Engineering, Ahmadu Bello University, Zaria, Nigeria Email: ezeval7@yahoo.com

A. B. Bababe, Department of Computer Science & Engineering, Sharda University, Greater Noida, India. Email: bababeadam@gmail.com

© The Authors. Published by Blue Eyes Intelligence Engineering and Sciences Publication (BEIESP). This is an [open access](#) article under the CC-BY-NC-ND license <http://creativecommons.org/licenses/by-nc-nd/4.0/>

Use of controlled validating environments like 20-sim this work which makes it efficient, fast and less susceptible to modelling errors as energy and information flow are captured[10].

The bond graph model of the DC motor is as shown in Figure 1.

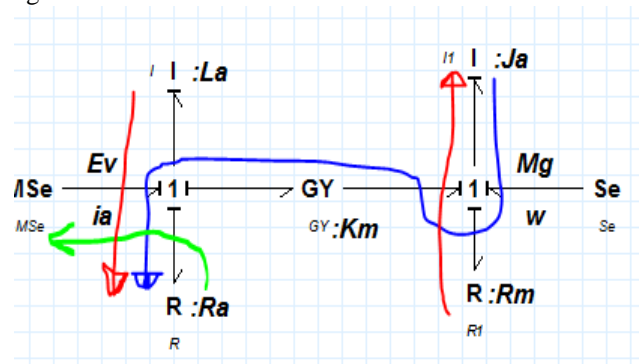


Figure 1: Bond Graph Model of DC Motor

In the bond graph model, the parameters are:

R: Ra Armature resistance

R: Rm Frictional coefficient

I: Ja Moment of Inertia

I: La Armature inductance

GY: Km Torque constant

Se: Source effort

M Se: Modulated Source effort

Assuming no bond loops and no open signal loops, the causal paths are depicted with the red, blue and green thin lines. Hence, the gains in association with these paths are derived as:

$$G_1 = -\frac{k_m^2}{(s^2 J_m I_a)} \quad (1.1)$$

$$G_2 = \frac{R_a}{s I_a} \quad (1.2)$$

$$G_3 = -\frac{R_m}{s J_m} \quad (1.3)$$

The resultant open loop model from the bond graph is determined as:

$$G_{open} = 1 + \frac{k_m^2}{s^2 J_m I_a} + \frac{R_a}{s I_a} + \frac{R_m}{s J_m} + \frac{R_a R_m}{s I_a s J_m} \quad (1.4)$$

The Transfer Function; G_{Tr} of the system according to Mason's rule derived between rotor shaft speed and applied armature voltage is therefore given by $I_a / E : s.t$



$$G_{Tr} = \frac{R_m + sJ_m}{R_a R_m + K_m^2 + (J_m R_a + I_a R_m)s + s^2 J_m I_a} \quad (1.5)$$

The relation between the position and the speed is given by $\theta(s) = \frac{1}{s}\omega(s)$ such that the resultant Transfer Function for the entire system is

$$\frac{\theta(s)}{V_a(s)} = \frac{R_m + sJ_m}{sR_a R_m + sK_m^2 + (J_m R_a + I_a R_m)s^2 + s^3 J_m I_a}$$

Where $V_a(s)$ is the applied voltage and $\theta(s)$ is the angle of displacement in Laplace transform. A simplified Transfer function (Laplace Transform) of the DC motor for easier analysis is given by [4] as

$$\frac{\theta(s)}{V_a(s)} = \frac{k}{s(1+s\tau)} \quad (1.7)$$

Where k and τ are the gain and time constant respectively.

III. EXPERIMENTAL SETUP OF MS 150 KIT

The MS 150 kits used for the laboratory experimental setup alongside a transfer function analyzer is shown in Fig. 1



Figure 2: MS 150 Kit Setup

The parameters obtained in the experiment includes:

- i. Potentiometer constant = 4.68V/rad
- ii. Tacho constant = 0.15V.s/rad
- iii. Sensitivity constant Kg = 2.7
- iv. Armature resistance = 7ohms
- v. Time constant t = 0.1785s
- vi. Velocity constant k = 10rad/v.s

The closed-loop of the system position control for this design is as shown in the block diagram of Figure 3.

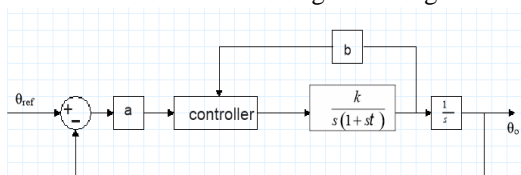


Figure 3: Block Diagram of Closed-Loop Controlled System

Considering the block diagram of the closed loop control system in fig 3, the system states space is given as:

$$\dot{x}_1 = \frac{a}{b} x_2 \quad (1.8)$$

$$\dot{x}_2 = \frac{1}{\tau}(bku - x_2) \quad (1.9)$$

Where $x_1 = a\theta$ and $x_2 = bw$. Also a and b are the gains of the angle and speed transducers (state variables) while u is the input signal.

IV. CONTROL SYSTEM DESIGN (1.6)

The controller is designed to achieve robust stability in the presence of variations due to inherent motor parameters while a good disturbance attenuation is maintained. The desired output was obtained by minimizing the errors between the referenced signal $e(t)$ and its time derivative $\dot{e}(t)$. This is mathematically stated as

$$U_{FC} = \Gamma(e, \dot{e}) \quad (1.10)$$

Where $\Gamma(\bullet)$ is a nonlinear fuzzy mapping function.

Table 1 is the presentation of linguistic variables used. A Triangular function was used for its simplicity in this work. The input/output is normalized between -1 and +1 using the scaling boxes of gains in the simulator. From the table 1, the “Ng” strongly affect the steady state error of the system while the “Pv” is to torque of the motor amidst disturbance. The rules commanding the fuzzy system response (output) are given in table 2. An intelligence in the design shows that the error between the reference and desired output and its derivative when “negative” and “zero”, respectively, the output of the fuzzy controller is a “slow” force. Mamdani method is chosen for design of fuzzy inference engine using “min-function” for “and-method”, “max-function” for “or-method”, and aggregation. The “centroid” was used for defuzzification; that is to transform the fuzzy output to a crisp output.

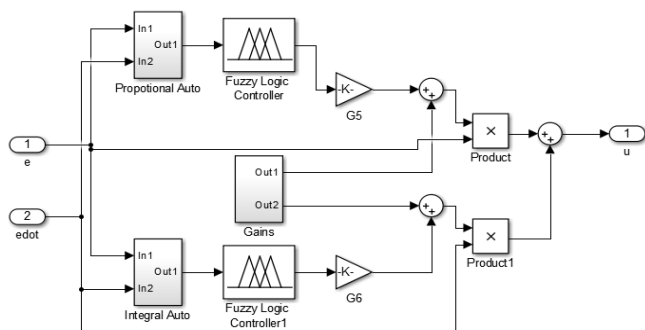
Table 1: Linguistic Variable for Input/Output

Ng	Negative
Ze	Zero
Pv	Positive

Table 2: Tabulated Fuzzy Rules

$e \setminus \dot{e}$	Ng	Ze	Pv
Ng	VerySlow	Slow	Slow
Ze	Slow	slow	Fast
Pv	Slow	Slow	Fast

The design of the fuzzy controller which incorporated automatic gain tuning and robust disturbance attenuation capabilities is shown in

**Figure 4: PD-Fuzzy Model with Automatic Gain**

Moreover, the standard PD CONTROL LAW:

$$U_T = u_1 + u_2 \quad (1.11)$$

Such that u_1 and u_2 are the proportional and integral control inputs respectively which are given as

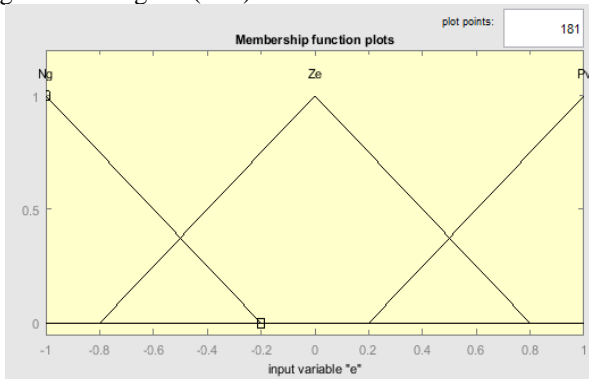
$$U_T(t) = (k_{po} + Fk_p)e(t) + (k_{Do} + Fk_D)\dot{e}(t) \quad (1.12)$$

Where the gains k_{po} and k_{Do} are gains fixed at 5000 and 10 respectively while the values of Fk_p and Fk_D are to be determined. The scaling gain factors that yielded the desired result obtained

$G_1 = 4e7, G_2 = 1250, G_3 = 8e6, G_4 = 250$, includes:

$$G_3 = 250, G_5 = 10e4, G_6 = 100$$

The error PD Fuzzy control responses are given from Figures 5 to Figures(5 - 8)

**Figure 5: Error MF for PD-Fuzzy Controller**

The error membership function variables are designed as layout in figure 5 above.

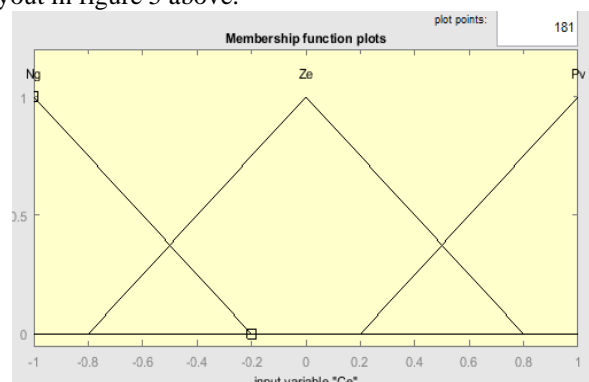
**Figure 6: Error Derivative MF for PD-Fuzzy Controller**

Figure 6, represents the derivative error membership function designed for this system

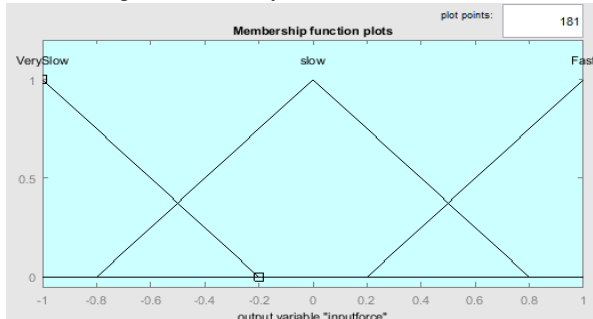
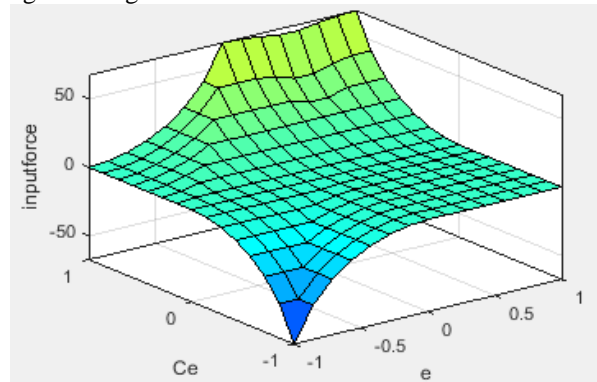


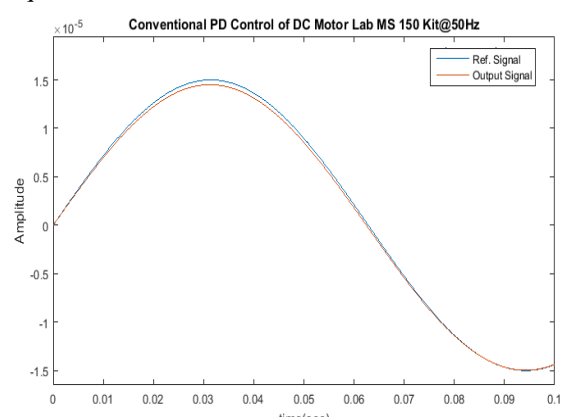
Figure 7: Output Response MF for PD-Fuzzy Controller
The output layout of the fuzzy linguistic variables is as designed in figure 7 above.

**Figure 8: Control Surface of Fuzzy-PD Controller**

The control surface in figure 8, shows the expected nonlinear mapping of the controlled system. The worst errors amount to less input force while the best values of minimization gives best input force.

V. SIMULATION RESULTS AND DISCUSSIONS

The simulation results are displayed in Figures [9 – 14]. The responses of the Fuzzy-PD controller and the conventional PD controller based on using sinusoidal signals of frequencies 50Hz, 100Hz and 500Hz. Hence:

**Figure 9: Conventional PD Control of DC Motor MS 150 Kit @50Hz**

Intelligent Control for Laboratory DC Motor

The response of the PD controller at a frequency of 50Hz. The gap between the referenced signal and the output is as shown in figure 9.

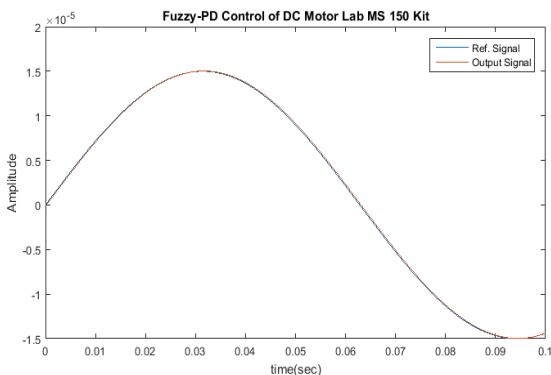


Figure 10: Fuzzy-PD Control of DC Motor MS 150 Kit @ 50Hz

Figure 10 shows the Fuzzy-PD controller response at 50Hz.

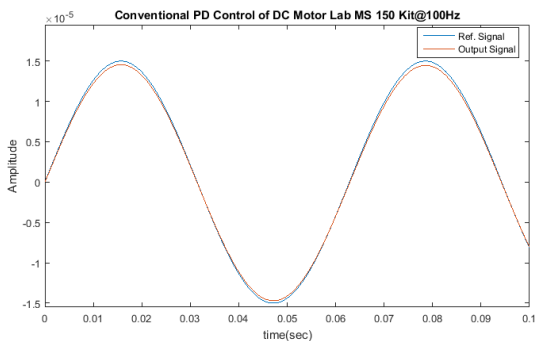


Figure 11: Conventional PD Control of DC Motor MS 150 Kit @ 100Hz

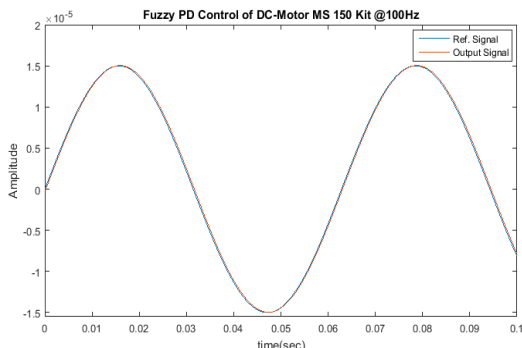


Figure 12: Fuzzy-PD Control of DC Motor MS 150 Kit @ 100Hz

Figure 12 shows the Fuzzy-PD controller response at 100Hz.

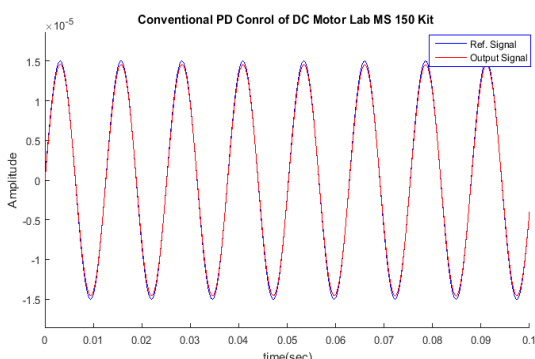


Figure 13: Conventional PD Control of DC Motor MS 150 Kit @ 500Hz

Figure 13 shows the Fuzzy-PD controller response at 50Hz.

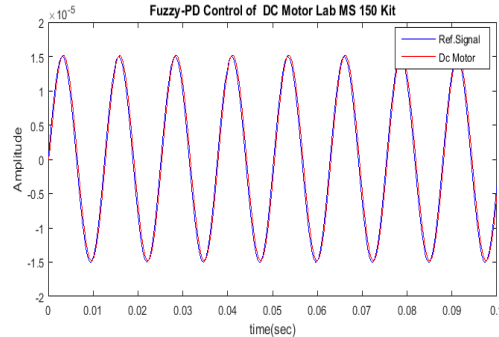


Figure 14: Fuzzy-PD Control of DC Motor MS 150 Kit @ 500Hz

Figure 14 shows the Fuzzy-PD controller response at 500Hz.

Table 3: Tracking -Error Performance for Sinusoidal Trajectory (%)

Freq(Hz)\Controller	Conv-PD	Fuzzy-PD
50Hz	0.014	0.013
100Hz	0.023	0.0134
500Hz	0.032	0.015

The performance of the Conventional PD and Fuzzy-PD minimization of error as shown in Table 3. affirms that the Fuzzy-PD yielded better expected performance.

VI. CONCLUSION

Fuzzy PD controller was designed for a DC motor (Lab MS 150 kit) Feedback laboratory setup. The performance of Fuzzy-PD controller had a consistent tracked best performance with a smaller tracking error compared to the performance of a conventional PD controller at frequencies of 50Hz, 100Hz and 500Hz respectively. The error margin from the various test shows that the Fuzzy-PD demonstrated could be a better choice of controller for a DC-motor application as its minimization of error in the tracking of the referenced signal for DC motor applications.

REFERENCE

1. T. Nishiyama, S. Suzuki, M. Sato, and K. Masui, "Simple Adaptive Control with PID for MIMO Fault Tolerant Flight Control Design," in AIAA Infotech@ Aerospace, ed, 2016, p. 0132.
2. G.-J. Su and J. W. McKeever, "Low-cost sensorless control of brushless DC motors with improved speed range," Power Electronics, IEEE Transactions on, vol. 19, pp. 296-302, 2004.
3. R. Saidur, S. Mekhilef, M. Ali, A. Safari, and H. Mohammed, "Applications of variable speed drive (VSD) in electrical motors energy savings," Renewable and Sustainable Energy Reviews, vol. 16, pp. 543-550, 2012.
4. R. Krishnan, Electric motor drives: modeling, analysis, and control: Prentice Hall, 2001.
5. N. Hemati, J. S. Thorp, and M. C. Leu, "Robust nonlinear control of brushless DC motors for direct-drive robotic applications," Industrial Electronics, IEEE Transactions on, vol. 37, pp. 460-468, 1990.
6. G.-R. Yu and R.-C. Hwang, "Optimal PID speed control of brush less DC motors using LQR approach," in Systems, Man and Cybernetics, 2004 IEEE International Conference on, 2004, pp. 473-478.
7. V. Vossos, K. Garbesi, and H. Shen, "Energy savings from direct-DC in US residential buildings," Energy and Buildings, vol. 68, pp. 223-231, 2014.



8. H. O. Ahmed, "Speed Sensorless Vector Control of Induction Motors Using Rotor Flux based Model Reference Adaptive System," Journal of Engineering and Computer Science, vol. 17, 2016.
9. W. Borutzky, Bond Graph Methodology. New York: Springer, 2010.
10. B. O. B. Arun K. Samantaray, A Bond Graph Approach, Model-based Process Supervision. Scotland, UK, 2008.